

A Fine-Grained Analysis of mmWave Heterogeneous Networks

Le Yang, Fu-Chun Zheng and Shi Jin

Abstract—A fine-grained analysis of the cache-enabled networks is crucial for system design. In this paper, we focus on the meta distribution of the signal-to-interference-plus-noise-ratio (SINR) in the mmWave heterogeneous networks where the base stations (BS) in each tier are modeled as Poisson point process (PPP). By utilizing stochastic geometry, we derive the moments of the conditional success probability, based on which the exact expression of meta distribution and its beta approximation are derived. In addition, key performance metrics, the success probability, the variance of the conditional success probability, the mean local delay and the network jitter are achieved. The distinguishing characteristics of the mmWave communications, including different path loss laws for line-of-sight and non-line-of-sight links and directional beamforming are incorporated into the analysis. The simulation results reveal the impact of the key network parameters, such as blockage parameter, bias factor, number of antenna elements and density on the performance.

Index Terms—Stochastic geometry, heterogeneous networks, millimeter wave, meta distribution, local delay.

I. INTRODUCTION

A. Motivation

Accompanying with the rapid proliferation of the communication and electronic technologies, various new applications have emerged, such as autonomous vehicles, virtual reality and augmented reality. As a result, the fifth generation (5G) and beyond 5G are anticipated to provide the massive connectivity for the enormous amount of services [1]. Specifically, the data rate demand of the virtual and augmented realities reaches the order of gigabit-per-second [2]. In order to meet the increasing data rate demand, millimeter wave (mmWave) communications stands out as a promising approaches to realize the gigabit data rate [3].

The mmWave spectrum corresponding from 30GHz to 300GHz has attracted considerable attention from both academia and industry due to the huge bandwidth. However, the mmWave communications suffer from several drawbacks, such as the high path loss caused by its susceptibility to the atmospheric absorption, diffraction and deflection and the poor penetration to the blockages [4]. Fortunately, these limitations could be overcome by deploying directional antennas. Channel measurements have shown that a transmission range of 150-200 meters can be achieved. In addition, much higher data rate and comparable coverage rather than the sub-6GHz networks can be obtained. Another important feature of the mmWave networks is the heterogeneity.

In general, a heterogeneous network consists of K network tiers distinguished by the spatial densities, the transmit powers and the blockage models [5], [6]. For example, the low-power

and high-density small-cell base stations (BSs) coexist with the high-power and low-density large-cell BSs. The small-cell BSs can offload some percentage of users from the congested large-cell BSs to improve the quality of service [7]. In order to alleviate the burden of the large-cell BSs, cell range expansion (CRE) technology can be utilized [8], [9]. In order to evaluate the performance of the mmWave heterogeneous networks, stochastic geometry is utilized as a powerful analyzing tool due to its capability of capturing the variability and irregularity of the node locations in real networks. However, the current analysis mainly focus on the performance of the typical user by spatial averaging. A important performance metric is the success probability, which is defined as the complementary cumulative density function (CCDF) of the signal-to-interference-ratio (SIR). The success probability is obtained by calculating the expectation of the conditional success probability over the underlying point processes modeling the locations of the BSs in all tiers. Therefore, it cannot reflect the performance variation for each individual link. Note that the real deployment of the mmWave heterogeneous networks concerned by the network operators are the questions such as “What fraction of users can achieve the STP of at least x (an arbitrary percentage value)?”. Unfortunately, the success probability only answers the question of “On average what fraction of users experience successful transmission?”. To overcome this drawback and obtained a fine-grained analysis on the SIR distribution, the meta distribution is introduced [19], which is defined as the CCDF of the success probability.

B. Related Works

The mmWave networks has been extensively investigated in the previous literatures by utilizing tools from stochastic geometry. The authors in [11] proposed a analytical framework to analyze the mmWave cellular networks. The expression of coverage probability and the achievable rate were derived and the simplified expression were obtained by utilizing the equivalent LOS ball model in the dense BS deployment scenario. In [12], the authors investigated the impact of the directional antenna arrays by proposing two antenna patterns with analytical tractability and desired accuracy to approximate the actual antenna pattern and derived the corresponding coverage probability in the mmWave ad hoc and cellular networks. In [13], two types of heterogeneity, i.e., spectrum heterogeneity and deployment heterogeneity, were considered in the mmWave networks. In spectrum heterogeneity, the users used the low frequencies for control message exchange while

the higher frequencies are used for the data communication. For deployment heterogeneity, two deployment scenarios, i.e., the stand-alone scenario and the integrated scenario, were introduced. All tiers operated in the mmWave frequency bands in the stand-alone scenario while the sub-6GHz networks coexisted with the mmWave networks in the integrated scenario.

The coverage probability of the stand-alone mmWave heterogeneous networks are studied by a variety of research works. In [10], the authors proposed a generalized mathematical framework for the analysis of the mmWave heterogeneous networks where the coverage probability and the average rate were obtained. In [11] and [10], a distance-dependent line-of-sight (LOS) probability function is utilized where the LOS and non-line-of-sight (NLOS) BSs are distributed as two independent Poisson point process (PPP). The LOS/NLOS state of each link is distinguished by the path loss model and the small-scale fading where the Nakagami fading with different parameters are assumed for LOS and NLOS links. In [14], the authors obtained the expression of the coverage probability and energy efficiency in the mmWave heterogeneous networks by utilizing multi-ball approximation for the blockage model. In [15], the authors proposed a low complexity BS selection scheme consisting of two-level procedures and provided the analytical and asymptotic expressions of the coverage probability corresponding to three BS pre-selection policies in the mmWave heterogeneous networks. In [16], the benefit of the BS cooperation in the downlink heterogeneous mmWave cellular networks is investigated.

The coverage or success probability of the coexisting sub-6GHz and mmWave networks has been analyzed in the previous literatures. In [17], the uplink-downlink signal-noise-ratio (SNR) and rate distribution of the self-backhaul mmWave cellular networks were theoretically elaborated. The authors in [18] characterized the uplink and downlink cell association strategies and demonstrated the superiority of the proposed decoupled cell association strategies over the traditional coupled approach in the hybrid networks where the sub-6GHz macro BSs coexisted with the mmWave small-cell BSs. Note that [17] and [18] utilized the Rayleigh fading as the small-scale fading for the analytical tractability.

The above works only analyze the coverage or success probability of the mmWave networks without delving into the performance variation for each link. To obtain a fine-grained analysis on the network performance, the meta distribution was proposed in [19]. The meta distribution of the cellular networks has been investigated extensively in previous works. In [19], where the moments of the conditional success probability, the exact expression and approximation of the meta distribution for the cellular networks and bipolar networks were derived, respectively. The exact analytical expressions and the beta approximations of the meta distribution have since been obtained in various other scenarios, including the heterogeneous networks [20], non-Poisson networks [21], D2D communications [22], coordinated multipoint transmission [23], non-orthogonal multi-access [24] and fractional power control [25]. In [26], the meta distribution and beta approximation of the SIR in the mmWave D2D networks was derived.

C. Contributions

Although the meta distribution of SIR is investigated in various previous works, the meta distribution in mmWave heterogeneous networks still remains to be studied. In this paper, we develop a meta distribution analytical framework for the mmWave heterogeneous networks. Unlike [26] where the simplified Rayleigh fading channel is assumed and [27] where the equivalent ball model is utilized to approximate the LOS probability for each link, we utilize the LOS probability function to approximate the LOS probability of each link and Nakagami fading with different parameters are assumed for the small-scale fading of LOS/NLOS links. Note that the Rayleigh fading is a special case of the Nakagami fading when the shape parameter equals to 1.

Our contribution are summarized as follows

- 1) Different from [10], [11] and [14] where only the approximation of the success probability in the mmWave heterogeneous networks are derived, we characterize the exact expression of the success probability for each tier. In addition, the simplified expression of the success probability under the special case where the blockage parameters are sufficiently small is derived.
- 2) The moments and the variance of the conditional success probability are derived when the user is associated with a LOS/NLOS BS in each tier. Based on the results from the moments of the conditional success probability, the exact expression and the beta approximation of the meta distribution of the SINR and the data rate are obtained. In addition, the mean local delay and the variance of the local delay (network jitter) are derived.
- 3) The numerical results reveal the effect of the directional antenna array gain on the variance of the success probability. The

II. SYSTEM MODEL

We consider a downlink scenario in the mmWave heterogeneous networks consisting of K tiers. Denote $\mathcal{K} \triangleq \{1, 2, \dots, K\}$. The BSs in each tier $k \in \mathcal{K}$ are assumed to be distributed as a homogeneous Poisson point process (PPP) Φ_k with density λ_k . The BSs in the k th tier transmit with power P_k . We assume that the BSs in all tiers operate over the same mmWave frequency band and the bandwidth is W . Without loss of generality, we study the performance of the typical user u_0 located at the origin according to Slivnyak's theorem [28].

The wireless channel in the mmWave network is characterized by the large-scale and small-scale fading. We first analyze the large-scale fading. Since the signal is sensitive to the blockages in the mmWave environment, the BSs can be line-of-sight (LOS) or non-line-of-sight (NLOS) based on that whether there is blockage intersecting the link between u_0 and the BS. If there is no blockage intersecting the link between the link between u_0 and the BS, the corresponding link is LOS. Otherwise, the link is NLOS. The probability that a link between u_0 and a BS located at distance x is considered to be LOS is defined as the LOS probability function $p_L x = e^{-\beta_k x}$, where β_k is the blockage parameter for the k th tier and determined by the average size and density of the blockages.

In addition, the probability that a link with length x is NLOS is given by $p_N(x) = 1 - p_L(x)$. The received signal is attenuated due to the path loss and the path loss exponent is utilized to measure the severity of the attenuation. To distinguish the LOS and NLOS states for an arbitrary link, different path loss laws is employed for the LOS and NLOS links as follows

$$L(x) = \begin{cases} \kappa_L x^{\alpha_L} & \text{with probability } p_L(x) \\ \kappa_N x^{\alpha_N} & \text{with probability } p_N(x) \end{cases} \quad (1)$$

where κ_L and κ_N are the intercepts for the LOS and NLOS link at 1 meter, α_L and α_N the path loss exponent for the LOS and NLOS link.

For the small-scale fading, we denote by $h_{k,i}$ the small-scale fading term of link i in the k th tier and assume Nakagami fading with the probability density function (PDF) $f(h) = \frac{2M_\rho^{M_\rho} h^{2M_\rho-1}}{\Gamma(M_\rho)} e^{-M_\rho h^2}$ for each link. Specifically, the Nakagami fading with parameter M_L and M_N is applied to the LOS and NLOS links, respectively. Therefore, $|h_{k,i}|^2$ is a Gamma distributed random variable. Note that the small-scale fading in mmWave networks is less severe than the sub-6GHz networks due to the directional antenna array and a large M_L can be utilized to approximate the fading with small variance for the LOS link. When $M_\rho = 1, \rho \in \{L, N\}$, the small-scale fading reduces to the Rayleigh fading. With the deployment of the antenna array, the BSs perform beamforming where the main lobe directs towards the dominant propagation path and the side lobes direct towards other directions. In addition, for analytical tractability, we utilize a sector model to approximate the array antenna pattern [29]-[31]. The beam direction of the interfering BSs is uniformly distributed on $[0, 2\pi]$. The antenna array gain between u_0 and an interfering BS is given by

$$G = \begin{cases} \Psi, & \text{with probability } \frac{\delta}{2\pi}, \\ \psi, & \text{with probability } \frac{1-\delta}{2\pi}, \end{cases} \quad (2)$$

where Ψ denotes the main lobe gain, ψ the side lobe gain, δ the half power beamwidth. We assume that the angle of arrival (AoA) can be estimated at the BS and the antenna orientation steering can be adjusted by utilizing the estimated AoA. Therefore, a perfect alignment is assumed between u_0 and its serving BS and the maximum array gain Ψ can be achieved for the link between u_0 and its serving BS.

u_0 is associated with the BSs providing the strongest signal power among all tiers. Note that the user association is jointly affected by the transmit power of the BS and the path loss of link between u_0 and the BS. Due to the LOS/NLOS state of the links between u_0 and the BSs, the nearest BS is not necessarily the BSs providing the strongest power in the k th tier. In addition, CRE is adopted to offload some user from the large-cell BSs to the small-cell BSs in order to alleviate the burden of the large-cell BSs and enhance the overall performance of the heterogeneous networks [8], [9]. Therefore, u_0 is associated with a BS based on the maximum biased received signal strength, which can be mathematically described as follows

$$P_k B_k G_k L_k(x)^{-1} > P_j B_j G_j L_{j,\min}(x)^{-1} \quad (3)$$

where $L_{j,\min}(x)$ denotes the minimum path loss between u_0 and the BSs in the j th tier.

The SINR is given by

$$\text{SINR} = \frac{P_k h_{k,0} L_k(x)^{-1}}{\sigma^2 + \sum_{j=1}^K \sum_{i \in \Phi_j \setminus B_{k,0}} P_j G_{j,i} h_{j,i} L_{j,i}^{-1}(x)} \quad (4)$$

where $G_{j,i}$, $h_{j,i}$ and $L_{j,i}$ denote array gain, small-scale fading and the path loss for the interfering link, the σ^2 the thermal noise. The meta distribution of the SINR $\bar{F}_{\mathcal{P}}(x)$ is defined as the complementary cumulative distribution function (CCDF) of the conditional success probability

$$\mathcal{P}(\theta) = \mathbb{P}(\text{SIR} > \theta | \Phi), \quad (5)$$

which is the CCDF of the SIR for u_0 conditioned on the realization of Φ . Henceforth, the meta distribution is given by [19]

$$\bar{F}_{\mathcal{P}}(y) \triangleq \mathbb{P}(\mathcal{P}(\theta) > y), \quad y \in [0, 1]. \quad (6)$$

Due to the ergodicity of the point processes, the meta distribution can be regarded as the fraction of active links with the conditional success probability greater than x .

The expression of the meta distribution includes multi-order moments of the conditional success probability. Denoting the b -th moment of \mathcal{P} by M_b , we can derive the expression of meta distribution by utilizing the Gil-Pelaez theorem. The exact form of the meta distribution is complex and considerable time will be consumed to obtain the final results. In order to facilitate the analysis, the beta distribution is utilized to approximate the meta distribution by matching the first and second moments.

We also analyze the per-link delay consisting of two parts, i.e., the transmission delay and the queuing delay. the retransmission delay is the main component of the transmission delay, which is defined as the number of retransmissions needed until a successful transmission occurs [32]. It can also be called the local delay. We denoted the local delay by L and thus the mean local delay can be written as

$$\mathbb{E}[L] \stackrel{(a)}{=} \mathbb{E} \left[\frac{1}{\mathcal{P}(\theta)} \right] = M_{-1}. \quad (7)$$

where (a) follows from the fact that L is geometrically distributed with parameter $\mathcal{P}(\theta)$ conditioned on Φ . Denoting $L|\Phi$ by L_Φ , we have

$$\mathbb{P}(L_\Phi = k) = (1 - \mathcal{P})^{k-1} \mathcal{P}, \quad k \in \mathbb{N}. \quad (8)$$

where \mathcal{P} is the conditional success probability. As shown in (7), the mean local delay can be derived by computing the -1 -st moment of the conditional success probability.

III. AUXILIARY RESULTS

In this section, we first provide the characteristics of the path loss, i.e., the PDF and the complementary cumulative density function (CCDF) of the path loss, then provide the expression of the association probability. Let \mathcal{N}_k denote the point process of the path loss between u_0 and the BSs in the k th tier. Therefore, the CCDF and PDF of the path loss can be provided in the following lemma.

Lemma 1: The CCDF of the path loss between u_0 and its serving BS is given by

$$\bar{F}_{L_k}(x) = \exp(-\Lambda_k([0, x])), k \in \mathcal{K} \quad (9)$$

where $\Lambda_k([0, x])$ is defined as in (10) on the top of the next page.

$$\begin{aligned} \Lambda_k([0, x]) &= \pi \lambda_k (x/\kappa_N)^{2/\alpha_N} \\ &+ 2\pi \lambda_k \beta_k^{-2} \left(1 - e^{-\beta_k (x/\kappa_L)^{1/\alpha_L}} \left(1 + \beta_k (x/\kappa_L)^{1/\alpha_L} \right) \right) \\ &- 2\pi \lambda_k \beta_k^{-2} \left(1 - e^{-\beta_k (x/\kappa_N)^{1/\alpha_N}} \left(1 + \beta_k (x/\kappa_N)^{1/\alpha_N} \right) \right). \end{aligned} \quad (10)$$

Proof: See Appendix A.

Unlike the traditional sub-6GHz networks, the blockage parameter β_k plays an important role in determining the path loss between u_0 and its serving BS. The signal from the serving LOS BS attenuates faster than the NLOS BS. Next, we characterize the path loss between u_0 and its serving LOS/NLOS BSs.

Lemma 2: The CCDF of the path loss between u_0 and its serving LOS/NLOS BS in the k th tier is given by

$$\bar{F}_{L_{k,\rho}}(x) = \exp(-\Lambda_{k,\rho}([0, x])), k \in \mathcal{K}, \quad (11)$$

where $\rho \in \{\text{LOS}, \text{NLOS}\}$ and $\Lambda_{k,\rho}([0, x])$ corresponds to LOS and NLOS, respectively, as shown in (12) and (13).

$$\begin{aligned} \Lambda_{k,L}([0, x]) &= 2\pi \lambda_k \beta_k^{-2} \left(1 - e^{-\beta_k (x/\kappa_L)^{1/\alpha_L}} \left(1 + \beta_k (x/\kappa_L)^{1/\alpha_L} \right) \right) \end{aligned} \quad (12)$$

$$\begin{aligned} \Lambda_{k,N}([0, x]) &= \pi \lambda_k (x/\kappa_N)^{2/\alpha_N} \\ &- 2\pi \lambda_k \beta_k^{-2} \left(1 - e^{-\beta_k (x/\kappa_N)^{1/\alpha_N}} \left(1 + \beta_k (x/\kappa_N)^{1/\alpha_N} \right) \right) \end{aligned} \quad (13)$$

Proof: $\Lambda_{k,\text{LOS}}([0, x])$ and $\Lambda_{k,\text{NLOS}}([0, x])$ can be derived following the similar steps with the derivation of $\Lambda_k([0, x])$.

The PDF of the distance between u_0 and its serving BS is given by

$$f_{L_{k,\rho}} = -\frac{d\bar{F}_{L_{k,\rho}}(x)}{dx} = \Lambda'_{k,\rho}([0, x]) \exp(-\Lambda_{k,\rho}([0, x])) \quad (14)$$

By utilizing the derived results, we can obtain the expression of the association probability in the following lemma.

Lemma 3: The probability that u_0 is associated with the k th tier is given by

$$A_{k,\rho} = \int_0^\infty \Lambda_{k,\rho}([0, l_k]) e^{\sum_{j=1}^K \Lambda_j \left([0, \frac{P_j B_j G_j}{P_k B_k G_k} l_k] \right)} dl_k \quad (15)$$

Proof: See Appendix B.

From Lemma 3, we observe that the association probability is dependent on three sets of parameters, i.e., the physical layer parameters, the antenna array parameters and the mmWave environment parameters. The physical layer parameters include the transmit power P and the BS density λ_k . The antenna array parameters consist of the main lobe gain Ψ , the side lobe gain ψ and the half power beamwidth δ . The mmWave

environment parameters consist of the blockage parameters β_k and the path loss exponent $\alpha_\rho, \rho \in \{L, N\}$.

Note that the expression of the association probability is in a complex form. In order to obtain more insight on the effect of the network parameters on the probability that u_0 is associated with the k th tier, we simplify the expression by utilizing the step function to model the LOS probability of the links between u_0 and the BSs in the k th tier. In the step function model, we assume that R_k is the maximum length of an LOS link in the k th tier. In addition, the LOS probability is 1 for the BSs with the distance $(0, R_k]$ and 0 for the BSs with the distance (R_k, ∞) .

Corollary 1: In a two-tier network with the step function to model the LOS probability, the expression of the probability for u_0 to be associated with a LOS BS in the k th tier is given in (16) and (17), as shown at the top of the next page.

IV. ANALYSIS OF META DISTRIBUTION

In this section, we first provide the exact expression of the success probability, followed by the analytical expression of the moments of the conditional success probability, then the expression of the meta distribution of the SINR distribution is provided. Note that the approximation of the moments of the conditional success probability is also derived.

A. Moments of Conditional Success Probability

Theorem 1: Given that u_0 is associated with a LOS/NLOS BS in the k th tier, the success probability is given by

$$\mathcal{P}_{b,k,\rho} = \frac{1}{A_{k,\rho}} \int_0^\infty f_{L_{k,\rho}}(l_{k,\rho}) \|\exp(\mathbf{Q}_{M_\rho})\|_1 dl_{k,\rho} \quad (18)$$

where $\exp(\mathbf{A})$ is the matrix exponential, i.e., $\exp(\mathbf{A}) = \sum_{k=0}^\infty \frac{\mathbf{A}^k}{k!}$, $\|\cdot\|$ is the l_1 -induced norm, \mathbf{Q}_{M_ρ} is a $M_\rho \times M_\rho$ Toeplitz matrix

$$\mathbf{Q}_{M_L} = \begin{bmatrix} q_{k,0} & & & & \\ q_{k,1} & q_{k,0} & & & \\ \vdots & \vdots & \ddots & & \\ q_{M_\rho-1} & q_{M_\rho-2} & \cdots & q_{k,0} & \end{bmatrix}, \quad (19)$$

where $q_{k,0}$ and $q_{k,n}, n \in \{1, 2, \dots, M_\rho - 1\}$ is given in (20) and (21), as shown at the top of the next page. $(a)_n = a(a+1) \cdots (a+n-1)$ is the rising Pochhammer symbol [33].

$$q_{k,0} = \sum_{j=1}^K \sum_{\nu \in \{L, N\}} \sum_{G \in \{\Psi, \psi\}} \int_0^\infty \left(1 - \left(1 + \frac{\theta L_{k,\rho} M_\rho P_j G}{x P_k G_0 M_\nu} \right)^{-M_\nu} \right) \Lambda_{j,\nu}(dx) \quad (20)$$

$$\begin{aligned} q_{k,n} &= -\sigma^2 [2-n]^+ - \sum_{j=1}^K \sum_{\nu \in \{L, N\}} \sum_{G \in \{\Psi, \psi\}} \\ &\frac{(M_\nu - 1)_n P_j G \theta M_\rho L_{k,\rho}}{n! P_k G_0} \int_0^{\frac{B_k M_\rho}{B_j G_0}} \frac{x^{n-2}}{(1+x)^{M_\nu+n}} \Lambda_{j,\nu}(dx) \end{aligned} \quad (21)$$

Proof: See Appendix C.

$$A_{1,L} = \begin{cases} \frac{\lambda_1 P_1 G_1 B_1}{\sum_{j=1}^2 \lambda_j P_j G_j B_j} \left(1 - e^{-\frac{\pi R_1^2}{P_1 G_1 B_1} (\sum_{j=1}^2 \lambda_j P_j G_j B_j)} \right), & \text{if } \sqrt{\frac{P_1 G_1 B_1}{P_2 G_2 B_2}} R_2 > R_1 \\ \frac{\lambda_1 P_1 G_1 B_1}{\sum_{j=1}^2 \lambda_j P_j G_j B_j} \left(1 - e^{-\frac{\pi R_2^2}{P_2 G_2 B_2} (\sum_{j=1}^2 \lambda_j P_j G_j B_j)} \right) + e^{-\frac{\pi R_2^2}{P_2 G_2 B_2} \sum_{j=1}^2 \lambda_j P_j G_j B_j} - e^{-\pi \sum_{j=1}^2 \lambda_j R_j^2}, & \text{otherwise} \end{cases} \quad (16)$$

$$A_{2,L} = \begin{cases} \frac{\lambda_2 P_2 G_2 B_2}{\sum_{j=1}^2 \lambda_j P_j G_j B_j} \left(1 - e^{-\frac{\pi R_2^2}{P_2 G_2 B_2} (\sum_{j=1}^2 \lambda_j P_j G_j B_j)} \right), & \text{if } \sqrt{\frac{P_2 G_2 B_2}{P_1 G_1 B_1}} R_1 > R_2 \\ \frac{\lambda_1 P_1 G_1 B_1}{\sum_{j=1}^2 \lambda_j P_j G_j B_j} \left(1 - e^{-\frac{\pi R_1^2}{P_1 G_1 B_1} (\sum_{j=1}^2 \lambda_j P_j G_j B_j)} \right) + e^{-\frac{\pi R_1^2}{P_1 G_1 B_1} \sum_{j=1}^2 \lambda_j P_j G_j B_j} - e^{-\pi \sum_{j=1}^2 \lambda_j R_j^2}, & \text{otherwise} \end{cases} \quad (17)$$

From Theorem 1, we can observe that the expression of the success probability is in a complex form. The main challenge in the analysis of the multi-antenna networks lies in tackling the high-order derivatives of the Laplace transform. The method in [36], [34] is adopted to obtain the success probability as the ℓ -induced norm of a Toeplitz matrix representation. Compared with the Faà di Bruno's formula including a large number of products and summations in [37], the results in (18) is in a more compact form. Different from the heterogeneous networks consisting of BSs equipped with omnidirectional antennas [38], the success probability is dependent on not only the physical layer parameters of all tiers, i.e., the transmit power P_k , the BS density λ_k , but also the antenna array parameters. Note that the parameters related to the mmWave environment play an important role in determining the success probability.

Since both the impact of the LOS and NLOS BSs are considered, the expression in (18) is in a complex form including an integral. In order to facilitate the analysis, we provide the simplified expression of the success probability under the special case where the blockage parameter is sufficiently small.

Corollary 2: In the interference-limited mmWave heterogeneous networks where the blockage parameter for all tier is sufficiently small, i.e., $\beta_k \rightarrow 0, k \in \mathcal{K}$, given u_0 is associated with a LOS/NLOS BS, the success probability can be expressed as follows

$$\mathcal{P}_{k,\rho} = V \left\| \left(\sum_{j=1}^K T \mathbf{I} - \mathbf{G}_{M_L} \right)^{-1} \right\|_1 \quad (22)$$

where $V = \sum_{j=1}^N \lambda_j \left(\frac{P_j B_j}{P_k B_k} \right)^{\frac{2}{\alpha_L}}$, T is given by

$$T = \lambda_j \left(\frac{P_j B_j}{P_k B_k} \right)^{\frac{2}{\alpha_L}} {}_2F_1 \left(\frac{2}{\alpha_L}, M_L; 1 - \frac{2}{\alpha_L}; -\frac{\theta M_{k,L} B_k}{G_0 B_j} \right) \quad (23)$$

where \mathbf{I} is a $M_L \times M_L$ identity matrix, \mathbf{G}_{M_L} is a $M_L \times M_L$ Toeplitz matrix, which can be expressed as

$$G_{M_L} = \begin{bmatrix} g_{k,0} & & & \\ g_{k,1} & g_{k,0} & & \\ \vdots & \vdots & \ddots & \\ g_{M_L-1} & g_{M_L-2} & \cdots & g_{k,0} \end{bmatrix}, \quad (24)$$

$$g_{k,0} = \exp \left(-\pi \lambda_j \left(\frac{P_j B_j}{P_k B_k} \right)^{\frac{2}{\alpha_L}} \left({}_2F_1 \left(\frac{2}{\alpha_L}, M_L; 1 - \frac{2}{\alpha_L}; -\frac{\theta M_{k,L} B_k}{G_0 B_j} \right) - 1 \right) \right) \quad (25)$$

Note that ${}_2F_1(\cdot)$ is the Gauss hypergeometric function [33], *Proof:* See Appendix D.

Theorem 2: Given that u_0 is associated with a LOS/NLOS BS in the k th tier, the b -th moment of the conditional success probability is given by

$$\xi_{b,k,\rho} = \frac{1}{A_{k,\rho}} \int_0^\infty f_{L_{k,\rho}}(l_{k,\rho}) \left(\sum_{\tau_1=0}^b \sum_{\tau_2=0}^{M_\rho \tau_1} \binom{b}{\tau_1} \binom{M_\rho \tau_1}{\tau_2} (-1)^{\tau_1 + \tau_2} e^{-s \sigma^2 \zeta_\rho \tau_2} \prod_{j=1}^K \mathcal{L}_{I_{j,L}}(s \zeta_\rho \tau_2) \mathcal{L}_{I_{j,N}}(s \zeta_\rho \tau_2) \right) dl_{k,\rho} \quad (26)$$

where $\zeta_\rho = (M_\rho!)^{-1/M_\rho}$, $\mathcal{L}_{I_{j,\nu}}(s \zeta_\rho \tau_2), \nu \in \{L, N\}$ is given by

$$\mathcal{L}_{I_{j,\nu}}(s \zeta_\rho \tau_2) = \exp \left(\int_{\frac{P_j B_j}{P_k B_k} l_{k,\rho}}^\infty \left(1 - \left(1 + \frac{\theta L_{k,\rho} M_\rho P_j \zeta_\rho \tau_2}{x P_k G_0 M_\nu} \right)^{-M_\nu} \right) \Lambda_{j,\nu}(dx) \right) \quad (27)$$

Proof: See Appendix E.

With the moments of the conditional success probability for each tier, the b -th moment of the conditional success probability for overall networks is given by

$$\xi_b = \sum_{k=1}^K \sum_{\rho \in \{L, N\}} A_{k,\rho} \xi_{b,k,\rho} \quad (28)$$

By applying the Gil-Pelaez theorem, the meta distribution of the SIR for a CCU is given by

$$\bar{F}_{\mathcal{P}}(y) = \frac{1}{2} + \frac{1}{\pi} \int_0^\infty \frac{\mathcal{J}(e^{-jt} \log y \xi_{jt})}{t} dt, \quad (29)$$

where $\mathcal{J}(z)$ is the imaginary part of z . Since the numerical evaluation of (29) is cumbersome and it is difficult to obtain further insight, we utilize a beta distribution to approximate the

meta distribution by matching the first and second moments, which can be easily obtained from the result in (26):

$$\xi_1 = \sum_{k=1}^K \sum_{\rho \in \{L, N\}} \int_0^\infty f_{L_{k,\rho}}(l_{k,\rho}) \left(\sum_{\tau_2=1}^{M_\rho \tau_1} \binom{M_\rho}{\tau_2} (-1)^{\tau_2+1} \right) e^{-s\sigma^2 \zeta_\rho \tau_2} \prod_{j=1}^K \mathcal{L}_{I_{j,L}}(s\zeta_\rho \tau_2) \mathcal{L}_{I_{j,N}}(s\zeta_\rho \tau_2) dl_{k,\rho} \quad (30)$$

$$\xi_2 = \sum_{k=1}^K \sum_{\rho \in \{L, N\}} \int_0^\infty f_{L_{k,\rho}}(l_{k,\rho}) \left(2 \sum_{\tau_2=1}^{M_\rho \tau_1} \binom{M_\rho}{\tau_2} (-1)^{\tau_2+1} \right) e^{-s\sigma^2 \zeta_\rho \tau_2} \prod_{j=1}^K \mathcal{L}_{I_{j,L}}(s\zeta_\rho \tau_2) \mathcal{L}_{I_{j,N}}(s\zeta_\rho \tau_2) + \sum_{\tau_2=1}^{2M_\rho} \binom{2M_\rho}{\tau_2} (-1)^{\tau_2} e^{-s\sigma^2 \zeta_\rho \tau_2} \prod_{j=1}^K \mathcal{L}_{I_{j,L}}(s\zeta_\rho \tau_2) \mathcal{L}_{I_{j,N}}(s\zeta_\rho \tau_2) dl_{k,\rho} \quad (31)$$

By matching the variance and mean of the beta distribution, i.e., $\xi_2 - \xi_1^2$ and ξ_1 , the approximated meta distribution of the SIR can be given by

$$\bar{F}_{\mathcal{P}_{k,\rho}} \approx 1 - I_y \left(\frac{\xi_1 \beta}{1 - \xi_1}, \beta \right), \quad y \in [0, 1], \quad (32)$$

where

$$\beta = \frac{(\xi_1 - \xi_2)(1 - \xi_1)}{\xi_2 - \xi_1^2} \quad (33)$$

and $I_y(a, b)$ is the regularized incomplete beta function

$$I_y(a, b) \triangleq \frac{\int_0^y t^{a-1} (1-t)^{b-1} dt}{B(a, b)}. \quad (34)$$

B. Mean Local Delay

In this subsection, we first derive the mean local delay, then obtain the closed-form expression of the variance of the mean local delay, i.e., the network jitter.

Theorem 3: Given u_0 is associated with a LOS/NLOS BS in the k th tier, the mean local delay is given by

$$\xi_{-1,k,\rho} = \frac{1}{A_{k,\rho}} \int_0^\infty f_{L_{k,\rho}}(l_{k,\rho}) \left(\sum_{\tau_1=0}^\infty \sum_{\tau_2=0}^{M_\rho \tau_1} \binom{M_\rho \tau_1}{\tau_2} (-1)^{\tau_2} \right) e^{-s\sigma^2 \zeta_\rho \tau_2} \prod_{j=1}^K \mathcal{L}_{I_{j,L}}(s\zeta_\rho \tau_2) \mathcal{L}_{I_{j,N}}(s\zeta_\rho \tau_2) dl_{k,\rho} \quad (35)$$

Proof: See Appendix F.

Accordingly, we can obtain the expression of the -2 -nd moment of the conditional success probability as follows

$$\xi_{-2,k,\rho} = \frac{1}{A_{k,\rho}} \int_0^\infty f_{L_{k,\rho}}(l_{k,\rho}) \left(\sum_{\tau_1=0}^\infty \sum_{\tau_2=0}^{M_\rho \tau_1} \binom{M_\rho \tau_1}{\tau_2} (-1)^{\tau_2} \right) (\tau_1 + 1) e^{-s\sigma^2 \zeta_\rho \tau_2} \prod_{j=1}^K \mathcal{L}_{I_{j,L}}(s\zeta_\rho \tau_2) \mathcal{L}_{I_{j,N}}(s\zeta_\rho \tau_2) dl_{k,\rho}. \quad (36)$$

With the -1 -st and -2 -nd of the conditional success probability given u_0 is associated with a LOS/NLOS BS in each tier, the mean local delay and the -2 -nd moment of the conditional success probability are given by

$$\xi_{-1} = \sum_{k=1}^K \sum_{\rho \in \{L, N\}} A_{k,\rho} \xi_{-1,k,\rho} \quad (37)$$

$$\xi_{-2} = \sum_{k=1}^K \sum_{\rho \in \{L, N\}} A_{k,\rho} \xi_{-2,k,\rho} \quad (38)$$

Therefore, the network jitter can be obtained by computing $\xi_{-2} - \xi_{-1}^2$.

C. Moments of Conditional Rate Coverage

The data rate depends on the total number of users served by a BS simultaneously. The probability mass function (PMF) of the number is given by

$$U_{k,\Upsilon} \triangleq \frac{1}{\Gamma(v)} \left(\frac{\lambda_u x}{3.5 \lambda_k} \right)^{v-1} \frac{\Gamma(3.5+v)}{\Gamma(4.5)} \left(1 + \frac{\lambda_u x}{3.5 \lambda_k} \right)^{-3.5-v} \quad (39)$$

Theorem 4: Given that u_0 is associated with a LOS/NLOS BS in the k th tier, the b -th moment of the conditional rate coverage probability can be expressed as

$$\xi_{R,b,k,\rho} \approx \sum_{v=1}^\infty U_{k,\Upsilon} \xi_{b,k,\rho} \left(2^{\frac{v}{W}} - 1 \right) \quad (40)$$

Proof: Given that u_0 is associated with a BS in the k th tier, the conditional rate coverage probability is given by

$$\mathcal{P}(\epsilon) = \mathbb{P}(R_k > \tau|\Phi) \quad (41)$$

Therefore, the b -th moment of the conditional rate coverage probability in the k th tier is given by

$$\begin{aligned} \xi_{R,b,k,\rho}(\epsilon) &= \mathbb{E} \left[\mathbb{P}(R_k > \epsilon|\Phi)^b \right] \\ &= \mathbb{E}_{\Upsilon_k} \left[\mathbb{E} \left[\mathbb{P}(R_k > \epsilon|\Phi, \Upsilon_k)^b \right] \right] \\ &= \sum_{v=1}^\infty U_{k,\Upsilon} \mathbb{E} \left[\mathbb{P}(\text{SINR} > 2^{\frac{v}{W}} - 1|\Phi)^b \right] \\ &= \sum_{v=1}^\infty U_{k,\Upsilon} \xi_{b,k,\rho} \left(2^{\frac{v}{W}} - 1 \right) \end{aligned} \quad (42)$$

V. SIMULATION RESULTS

In this section, we consider a two-tier mmWave heterogeneous network, where the pico base station (PBS, Tier $k=2$) is overlaid with the micro base station (MBS, Tier $k=1$). The impact of the physical layer parameters on the association probability is provided. Then the impact of key network parameters on the mean and variance of the STP as well as the meta distribution are presented. Unless otherwise stated, the parameters are set as listed in the following table.

Fig. 1 plots the association probability as the function of the blockage parameter. It can be observed that the association probability decreases with the blockage parameter of the

TABLE I
SYSTEM PARAMETERS

Parameters	Values
Transmit power	$P_1 = 43\text{dBm}, P_2 = 33\text{dBm}$
Bias factor	$B_1 = 1, B_2 = 1$
Path loss exponent	$\alpha_L = 2, \alpha_N = 4$
Density	$\lambda_1 = 5/(500^2\pi), \lambda_2 = 10/(500^2\pi)$
Blockage parameter	$\beta_1 = 0.006, \beta_2 = 0.024$
Nakagami parameter	$\rho_L = 3, \rho_N = 2$
Bandwidth	$W = 1\text{G}$
Carrier frequency	28GHz
$\kappa_L = \kappa_N$	$(F_c/4\pi)^2$
Zipf exponent	$\delta = 0.6$
Caching capacity	$F = 50, C_1 = 35,$ $C_2 = 25, C_3 = 15$

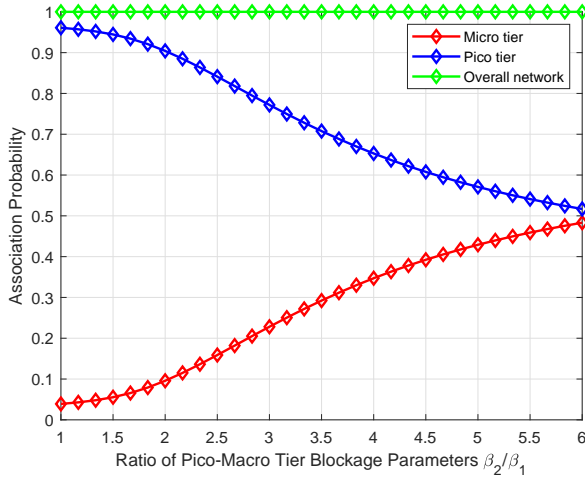
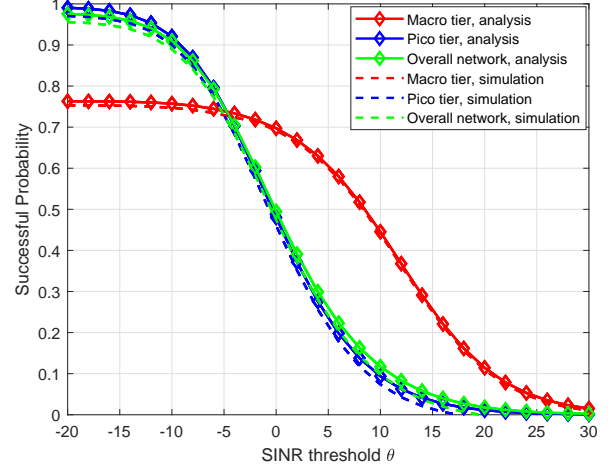


Fig. 1. Association Probability versus ratio of micro-pico tier blockage parameters β_2/β_1 .

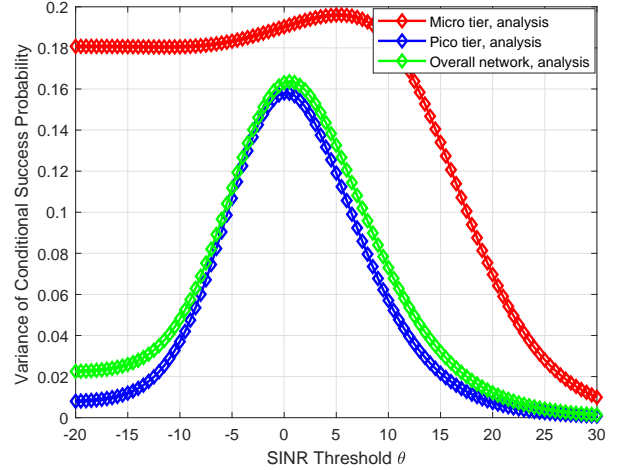
associated tier. The explanation can be stated as follows. When the blockage parameter increases, the probability that the serving BS is LOS decreases and signal power received from the serving BS may be decreased, thereby leading to the reduction of the association probability.

Fig. 2 plots the mean and variance of the success probability as the function of the SINR threshold θ . The simulation results match the theoretical analysis well. The performance fluctuation can be reflected by the variance of the STP. A large variance corresponds to a large performance fluctuation and vice versa [?]. From Fig. 2(a), it can be observed that the STP decreases with the SINR. From Fig. 2(b), we can observe that there exists a maximum variance for both tiers. The θ corresponding to the maximum for the pico tier is almost identical to that of the overall network.

Fig. 3 shows the impact of the density on the mean and variance of the success probability. From Fig. 3(a), it can be observed that when the density of pico tier increases, the success probability increases at start, then decrease gradually. The reason is that increasing the density of the pico tier motivates more users to be associated with the pico tier. Hence both the PBSs and MBSs have more per-user resources, resulting in a better performance. However, when the density of the pico tier further increases, the inter-tier interference



(a) Success probability versus SINR threshold



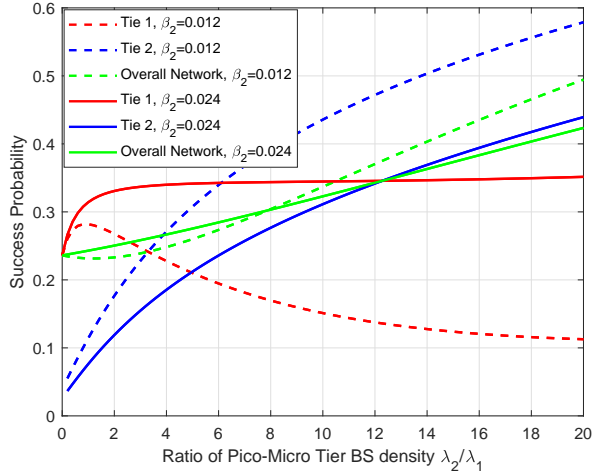
(b) Variance of versus SINR threshold.

Fig. 2. The impact of SINR threshold θ on the per-tier success probability and the variance.

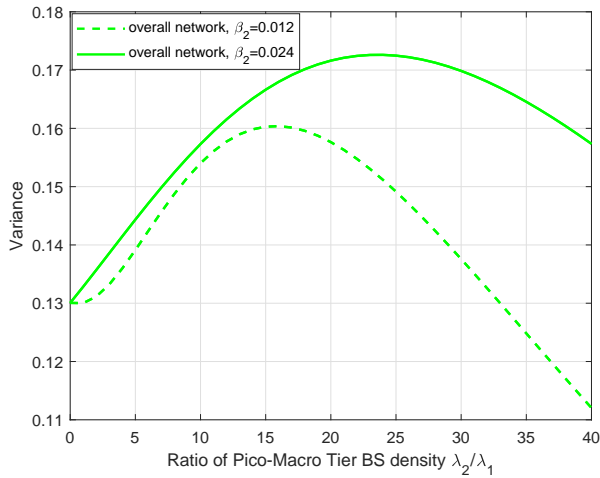
experienced by u_0 increases and the performance of the micro tier degrades. It is also noteworthy that the success probability for the pico tier decreases with the blockage parameter of the pico tier β_2 . Meanwhile, the success probability for the micro tier increases. This is because the probability that the serving BS is LOS decreases with β_2 , causing a degradation of the inter-tier interference and the signal power experienced by u_0 . We can observe from Fig. 3(b) that there exist a maximum variance of the success probability and the variance increases with β_2 . In addition, the value of λ_2/λ_1 corresponding to the maximum increases with β_2 .

Fig. 4 plots the mean and variance of the success probability as the function of the number of antenna elements N . From Fig. 4(a), we can observe the success probability increases with N . The reason is that the signal power is enhanced with a larger number of antenna elements. From Fig. 4(b), we can observe there exists a maximum variance and the value of θ corresponding to the maximum increases with N .

Fig.5 shows the impact of the bias factor of the pico tier



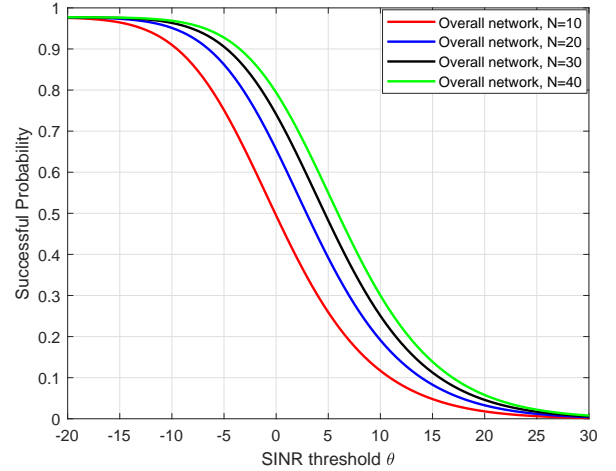
(a) Success probability versus the ratio of pico-micro tier densities under different blockage parameters for the pico tier.



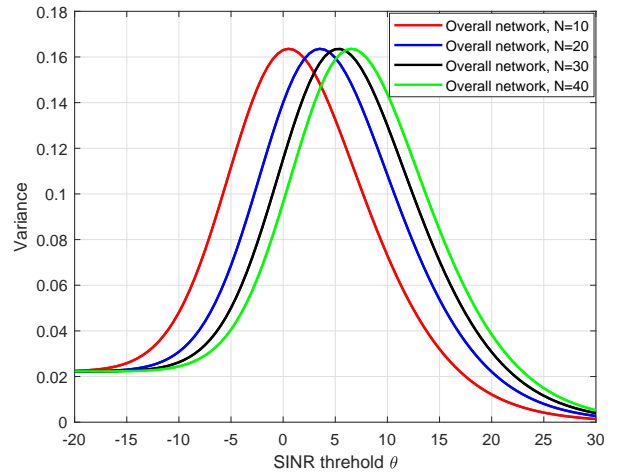
(b) Variance versus the ratio of pico-micro tier densities under different blockage parameters for the pico tier.

Fig. 3. The impact of the density of the pico tier λ_2 on the per-tier success probability and the variance.

B_2 on the mean and variance of the success probability under different ratios of pico-micro tier densities. From 5(a), it can be observed that success probability for the micro tier increases with B_2 . Meanwhile, the success probability of the overall network decreases. This can be explained as follows. When the bias factor of the pico tier increases, more users are offloaded to the pico tier and the MBSs have more per-user resources, resulting in a better performance. However, with biasing, users are associated with the BSs not providing the strongest received signal power, leading to a slight decrease in the overall network performance. From 5(b), we observe that variance of the success probability decreases with B_2 . In addition, the variance of success probability for the ratio of pico-micro tier densities $\lambda_2/\lambda_1 = 10$ is larger than that for $\lambda_2/\lambda_1 = 5$. This phenomenon indicates that compared with increasing the density of the PBSs, offloading the users to the pico tier by biasing can reduce the performance fluctuation while only causing a slight degradation of the overall network



(a) Success Probability versus SINR threshold under different number of antenna elements



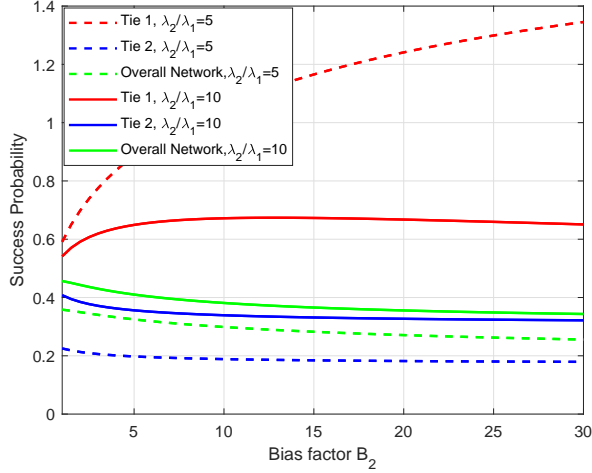
(b) Variance versus SINR threshold under different number of antenna elements.

Fig. 4. The impact of the number of antenna elements N on the per-tier success probability and the variance.

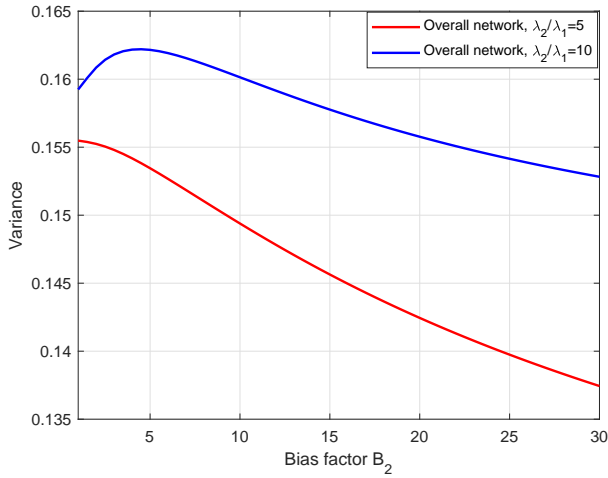
performance.

Fig. 6 analyzes the impact of the number of antenna element N on meta distribution of the SINR. The results is consistent with that in Fig. 4. With larger N , the proportion of the users with higher success probability increases. Fig. 7 plots the meta distribution of the SINR as the function of y under different blockage parameters of the pico tier. We observe that the proportion of the users with higher success probability decreases with the blockage parameter of the pico tier β_2 . We take $y = 0.5$ for example. When $\beta_2 = 0.006$, more than 70% users achieve the success probability of at least 0.5. However, when β_2 increase to 0.036, 52% users can achieve the success probability of at least 0.5.

Fig. 8 plots the mean local delay as the function of the ratio of the pico-micro tier densities λ_2/λ_1 . It can be observed that there exists a maximum local delay for the pico tier and the overall network. In addition, the mean local delay for the micro tier decreases with λ_2/λ_1 . The reason is that the more user are motivated to be associated with the pico tier when λ_2/λ_1



(a) Success probability versus bias factor under different ratio of pico-micro tier densities



(b) Variance versus bias factor under different ratio of pico-micro tier densities.

Fig. 5. The impact of bias factor the pico tier B_2 on the per-tier success probability and the variance.

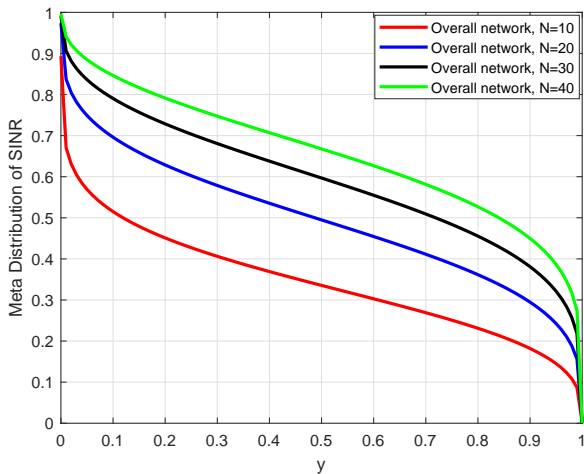


Fig. 6. Meta distribution versus y under different numbers of antenna elements N .

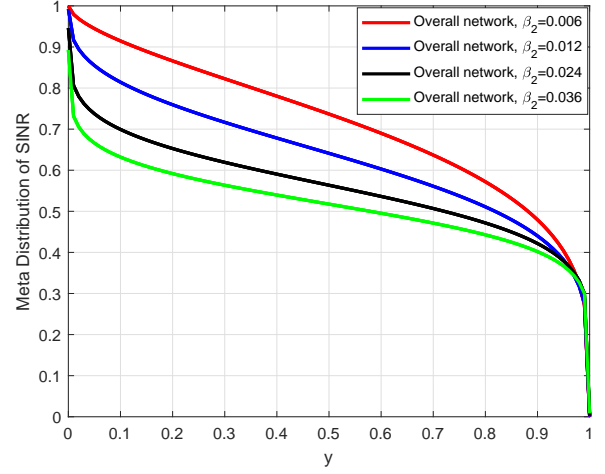


Fig. 7. Meta distribution versus y under different blockage parameters of the pico tier.

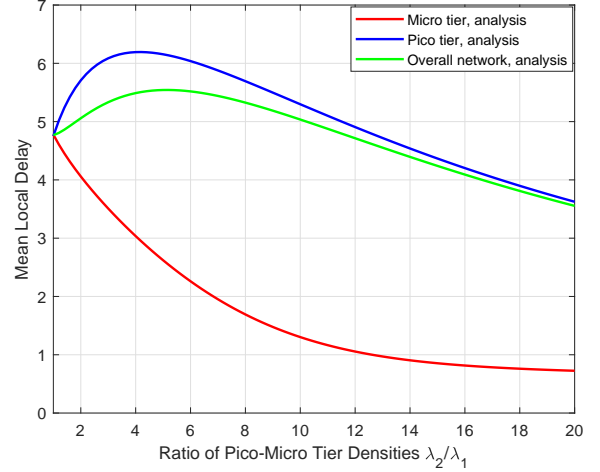


Fig. 8. Mean local delay versus ratio of pico-micro tier densities.

increases. Therefore, the MBSs have more per-user resources and the users are served more timely.

VI. CONCLUSION

We focus on the meta distribution of the SINR in the mmWave heterogeneous networks. By utilizing stochastic geometry, we derive the moments of the conditional success probability, based on which the exact expression of meta distribution and its beta approximation are derived. In addition, key performance metrics, the success probability, the variance of the conditional success probability, the mean local delay and the network jitter are achieved.

VII. APPENDIX

A. Proof of Lemma 1

The intensity measure for the BSs caching File f in the k th tier under LOS probability function model can be computed

as

$$\begin{aligned}
\Lambda_k([0, x]) &= \int_0^{(x/\kappa_L)^{1/\alpha_L}} 2\pi\lambda_k v e^{-\beta_k v} dv \\
&+ \int_0^{(x/\kappa_N)^{1/\alpha_N}} 2\pi\lambda_k v (1 - e^{-\beta_k v}) dv \\
&= \pi\lambda_k (x/\kappa_N)^{2/\alpha_N} \\
&+ 2\pi\lambda_k \beta_k^{-2} \left(1 - e^{-\beta_k (x/\kappa_L)^{1/\alpha_L}} \left(1 + \beta_k (x/\kappa_L)^{1/\alpha_L} \right) \right) \\
&- 2\pi\lambda_k \beta_k^{-2} \left(1 - e^{-\beta_k (x/\kappa_N)^{1/\alpha_N}} \left(1 + \beta_k (x/\kappa_N)^{1/\alpha_N} \right) \right). \tag{43}
\end{aligned}$$

$\Lambda'([0, x])$ can be obtained by computing the derivative of $\Lambda([0, x])$ as follows

$$\begin{aligned}
\Lambda'([0, x]) &= 2\pi\lambda_k \alpha_L^{-1} \kappa_L^{-2/\alpha_L} x^{2/\alpha_L - 1} e^{-\beta_k (x/\kappa_L)^{1/\alpha_L}} \\
&+ 2\pi\lambda_k \alpha_N^{-1} \kappa_N^{-2/\alpha_N} x^{2/\alpha_N - 1} \left(1 - e^{-\beta_k (x/\kappa_N)^{1/\alpha_N}} \right) \tag{44}
\end{aligned}$$

B. Proof of Lemma 3

The association probability is

$$\begin{aligned}
A_{k,\rho} &= \mathbb{P} \left(P_k G_k L_{k,\rho}^{-1} \geq \max_{j,j \neq k} P_j G_j L_j^{-1} \right) \\
&\times \mathbb{P}(L_{k,\bar{\rho}} > L_{k,\rho}) \\
&= \int_0^\infty \mathbb{P} \left(P_k G_k L_{k,\rho}^{-1} \geq \max_{j,j \neq k} P_j G_j L_j^{-1} \middle| l_{k,\rho} \right) \\
&\times \mathbb{P}(L_{k,\bar{\rho}} > L_{k,\rho} | l_{k,\rho}) f_{L_{k,\rho}}(l_{k,\rho}) dl_{k,\rho} \\
&= \int_0^\infty \prod_{j=1, j \neq k}^K \mathbb{P}(P_k G_k L_{k,\rho}^{-1} \geq P_j G_j L_{j,\rho}^{-1} | l_{k,\rho}) \\
&\mathbb{P}(L_{k,\bar{\rho}} > L_{k,\rho} | l_{k,\rho}) f_{L_{k,\rho}}(l_{k,\rho}) dl_{k,\rho} \\
&= \int_0^\infty e^{-\sum_{j=1, j \neq k}^K \Lambda_j \left([0, \frac{P_j G_j}{P_k G_k} l_{k,\rho}] \right)} e^{-\Lambda_{k,\bar{\rho}}([0, l_{k,\rho}])} \\
&\times \Lambda'_{k,\rho}([0, l_{k,\rho}]) e^{-\Lambda_{k,\rho}([0, l_{k,\rho}])} dl_{k,\rho} \\
&= \int_0^\infty \Lambda'_{k,\rho}([0, l_{k,\rho}]) e^{-\sum_{j=1}^K \Lambda_j \left([0, \frac{P_j G_j}{P_k G_k} l_{k,\rho}] \right)} dl_{k,\rho}, \tag{45}
\end{aligned}$$

where $\rho, \bar{\rho} \in \{\text{LOS}, \text{NLOS}\}$ and $\rho \neq \bar{\rho}$.

C. Proof of Theorem 1

Given that u_0 is associated with a LOS/NLOS BS in the k th tier, the success probability can be expressed as

$$\begin{aligned}
\mathcal{P}_{k,\rho} &= \mathbb{P} \left(\frac{P_k G_0 h_{k,0} L_k^{-1}(r)}{\sigma^2 + I} > \theta \right) \\
&= \mathbb{E}_{I,s} \left[\frac{\Gamma(M_\rho, s(\sigma^2 + I))}{\Gamma(M_\rho)} \right] \\
&= \sum_{m=0}^{M_\rho - 1} \mathbb{E}_{I,s} \left[e^{-s(\sigma^2 + I)} \frac{(s(\sigma^2 + I))^m}{m!} \right] \tag{46} \\
&= \mathbb{E}_s \left[\sum_{m=0}^{M_\rho - 1} \frac{(-s)^m}{m!} \mathcal{L}^{(m)}(s) \right]
\end{aligned}$$

where $\mathcal{L}(s)$ is the Laplace transform of the interference and the superscript (m) denotes the m -th derivative

of $\mathcal{L}(s)$. Due to the independence of K tiers, $\mathcal{L}(s)$ can be expressed as follows

$$\mathcal{L}(s) = \exp(-s\sigma^2) \prod_{j=1}^K \mathcal{L}_{I_{j,L}}(s) \mathcal{L}_{I_{j,N}}(s) \tag{47}$$

We first compute the Laplace transform of the LOS interfering BSs $\mathcal{L}_{j,L}(s)$ as follows

$$\begin{aligned}
\mathcal{L}_{I_{j,L}}(s) &= \mathbb{E} \left[\exp \left(-s \left(\sum_{i \in \Phi_j \setminus x_0} P_j h_{j,i} L_{j,i}^{-1} \right) \right) \right] \\
&= \prod_{i \in \Phi_j \setminus x_0} \mathbb{E} \left[\exp(-s P_j h_{j,i} L_{j,i}^{-1}) \right] \\
&= \prod_{i \in \Phi_j \setminus x_0} \frac{1}{\left(1 + \frac{s P_j}{M_L} L_{j,i}^{-1} \right)^{M_L}} \\
&= \exp \left(- \int_{\frac{P_j B_j}{P_k B_k} l_{k,\rho}}^\infty \left(1 - \left(1 + \frac{s P_j}{M_L} x^{-1} \right)^{-M_L} \right) \Lambda_{j,\rho}(dx) \right) \tag{48}
\end{aligned}$$

Note that $\mathcal{L}_{j,N}(s)$ can be obtained following the similar steps. Let $\mathcal{L}(s) = \exp(\eta(s))$ and we have $\mathcal{L}^{(1)}(s) = \eta^{(1)}(s) \mathcal{L}(s)$. Therefore, $\mathcal{L}^{(m)}(s)$ can be derived recursively following the formula of Leibniz for the product of two functions, which is given by

$$\mathcal{L}^{(m)}(s) = \frac{d^{m-1}}{ds} \mathcal{L}^{(1)}(s) = \sum_{n=0}^{m-1} \binom{m-1}{n} \eta^{(m-n)}(s) \mathcal{L}^{(n)}(s), \tag{49}$$

where the n -th derivative of the $\eta(s)$ is given by

$$\begin{aligned}
\eta^{(n)}(s) &= -\sigma^2 [2-n]^+ - \sum_{j=1}^K \sum_{\nu \in \{L, N\}} \int_{\frac{P_j B_j}{P_k B_k} l_{k,\rho}}^\infty \\
&(-1)^n (M_\nu)_n (P_j x^{-\alpha})^n (1 + s P_j x^{-\alpha})^{-M_\nu - n} \Lambda_{j,\nu}(dx) \\
&= -\sigma^2 [2-n]^+ - \sum_{j=1}^K \sum_{\nu \in \{L, N\}} (-1)^n (M_\nu - 1)_n P_j s^{1-n} \\
&\int_0^{\frac{B_k M_\rho}{B_j G_0}} \frac{t^{n-2}}{(1+t)^{M_\nu + n}} \Lambda_{j,\nu}(dt) \tag{50}
\end{aligned}$$

Letting $x_m = \frac{1}{n!} (-s)^n \mathcal{L}^{(n)}(s)$, the success probability can be rewritten as

$$\mathcal{P}_{k,\rho} = \mathbb{E} \left[\sum_{m=0}^{M_\rho - 1} x_m \right]. \tag{51}$$

Substituting $x_m = \frac{1}{n!} (-s)^n \mathcal{L}^{(n)}(s)$ into (50), we have

$$x_m = \sum_{n=0}^{m-1} \frac{m-n}{m} \left(\frac{(-s)^{m-n}}{(m-n)!} \eta^{(m-n)}(s) \right) x_n, \tag{52}$$

Letting $q_{k,n} \triangleq \frac{(-s)^n}{n!} \eta^{(n)}(s)$, the recursive relationship of x_m in (52) can be rewritten as $x_m = \sum_{n=0}^{m-1} \frac{m-n}{m} q_{k,m-n} x_n$. In order to solve x_m , two power series are defined as follows

$$Q(z) \triangleq \sum_{m=0}^{\infty} q_{k,m} z^m, \quad X(z) \triangleq \sum_{m=0}^{\infty} x_m z^m \tag{53}$$

It can be easily verified that $X^{(1)}(z) = Q^{(1)}(z)X(z)$. In addition, we have $X(0) = \exp(Q(0))$. Therefore, the solution of (53) is

$$X(z) = \exp(Q(z)) \quad (54)$$

Combining (60), (53) and (54), we have

$$\begin{aligned} \mathcal{P}_{k,\rho} &= \mathbb{E} \left[\sum_{m=0}^{M_\rho-1} x_m \right] = \mathbb{E} \left[\sum_{m=0}^{M_\rho-1} \frac{1}{m!} X^{(m)}(z) \Big|_{z=0} \right] \\ &= \mathbb{E} \left[\sum_{m=0}^{M_\rho-1} \frac{1}{m!} \frac{d^m}{dz^m} e^{Q(z)} \Big|_{z=0} \right] \end{aligned} \quad (55)$$

From [?] and [35], the first M_ρ coefficients of $\exp(Q(z))$ form the first column of $\exp(\mathbf{Q}_{M_\rho})$. Therefore, the success probability is given by

$$\mathcal{P}_{k,\rho} = \mathbb{E} \left[\left\| \exp(\mathbf{Q}_{M_\rho}) \right\|_1 \right]. \quad (56)$$

D. Proof of Corollary 2

Given that u_0 is associated with a LOS/NLOS BS in the k th tier, the success probability can be obtained following the similar steps with the proof of Theorem 1. The only difference lies in that the interference from the NLOS BSs and the noise can be neglected and $\mathcal{L}(s)$ can be expressed as follows

$$\mathcal{L}(s) = \prod_{j=1}^K \mathcal{L}_{I_j,L}(s) \quad (57)$$

We first compute the Laplace transform of the LOS interfering BSs $\mathcal{L}_{j,L}(s)$ as follows

$$\begin{aligned} \mathcal{L}_{I_j,L}(s) &= \exp \left(-\frac{2\pi\lambda_j}{\alpha_L \kappa^{\alpha_L}} \right. \\ &\quad \left. \int_{\frac{P_j B_j}{P_k B_k} l_{k,L}}^{\infty} \left(1 - (1 + s P_j x^{-1})^{-M_\rho} \right) x^{\frac{2}{\alpha_L} - 1} dx \right) \\ &= \exp \left(-\pi\lambda_j \left(\frac{P_j B_j L_{k,L}}{P_k B_k \kappa_L} \right)^{\frac{2}{\alpha_L}} \right. \\ &\quad \left. \left({}_2F_1 \left(\frac{2}{\alpha_L}, M_\rho; 1 - \frac{2}{\alpha_L}; -\frac{\theta M_{k,L} B_k}{G_0 B_j} \right) - 1 \right) \right) \end{aligned} \quad (58)$$

where the last equation follows from [33]. Then $\mathcal{L}(s)$ can be expressed as

$$\mathcal{L}(s) \stackrel{(a)}{=} \exp \left(-\pi \left(\frac{L_{k,L}}{\kappa_L} \right)^{\frac{2}{\alpha_L}} \left(\sum_{j=1}^K T - V \right) \right) \quad (59)$$

where (a) follows from $V = \sum_{j=1}^N \lambda_j \left(\frac{P_j B_j}{P_k B_k} \right)^{\frac{2}{\alpha_L}}$ and T is given in (23).

Letting $y_m = \frac{1}{n!} (-s)^n \mathcal{L}^{(n)}(s)$, the success probability can be rewritten as

$$\mathcal{P}_{k,\rho} = \mathbb{E} \left[\sum_{m=0}^{M_\rho-1} y_m \right]. \quad (60)$$

Substituting $x_m = \frac{1}{n!} (-s)^n \mathcal{L}^{(n)}(s)$ into (50), we have

$$y_m = \sum_{n=0}^{m-1} \frac{m-n}{m} g_{k,m-n} y_n. \quad (61)$$

where $g_{k,n}$ is given in (25). Let $g_{k,0} = \sum_{j=1}^K W$, $G(z) \triangleq \sum_{m=0}^{\infty} g_{k,m} z^m$ and $Y(z) \triangleq \sum_{m=0}^{\infty} y_m z^m$. From 61, we have

$$Y^{(1)}(z) = \pi G^{(1)}(z) Y(z) \quad (62)$$

The solution of (62) is $Y(z) = C \exp \left(\pi \left(\frac{L_{k,L}}{\kappa_L} \right)^{\frac{2}{\alpha_L}} G(z) \right)$. Then it remains to calculate C . From $Y(0) = y_0 = \mathcal{L}(s)$, which is given in (59) and $G(0) = g_{k,0}$, C can be obtained and $Y(z)$ is given by

$$Y(z) = \exp \left(\pi \left(\frac{L_{k,L}}{\kappa_L} \right)^{\frac{2}{\alpha_L}} (G(z) + V - 2g_{k,0}) \right) \quad (63)$$

Since the PDF of $L_{k,L}$ is given by

$$\begin{aligned} f_{L_{k,L}}(x) &= 2\pi \left(\frac{x}{\kappa_L} \right)^{\frac{1}{\alpha_L}} \left(\sum_{j=1}^K \lambda_j \left(\frac{P_j B_j}{P_k B_k} \right)^{\frac{2}{\alpha_L}} \right) \\ &\quad \exp \left(-\pi \left(\frac{x}{\kappa_L} \right)^{\frac{2}{\alpha_L}} \left(\frac{P_j B_j}{P_k B_k} \right)^{\frac{2}{\alpha_L}} \right) \end{aligned} \quad (64)$$

Therefore, $\mathbb{E}_{L_{k,L}}[Y(z)]$ can be obtained as

$$\mathbb{E}_{L_{k,L}}[Y(z)] = \frac{V}{2g_{k,0} - G(z)}. \quad (65)$$

Then we have

$$\mathbf{P} = V \sum_{m=0}^{M_L-1} \frac{1}{m!} \frac{d^m}{dz^m} \left(\frac{1}{2g_{k,0} - G(z)} \right) \Big|_{z=0}. \quad (66)$$

E. Proof of Theorem 2

Given that u_0 is associated with a LOS/NLOS BS in the k th tier, the b -th moment of the conditional success probability can be expressed as

$$\begin{aligned} \xi_{b,k,\rho} &= \mathbb{P} \left(\frac{P_k G_0 h_{k,0} L_k^{-1}(x)}{\sigma^2 + I} > \theta \right)^b \\ &= \mathbb{E}_{I,s} \left[\left(\frac{\Gamma(M_\rho, s(\sigma^2 + I))}{\Gamma(M_\rho)} \right)^b \right] \\ &\stackrel{(a)}{=} \mathbb{E}_{I,s} \left[\left(1 - \frac{\gamma(M_\rho, s(\sigma^2 + I))}{\Gamma(M_\rho)} \right)^b \right] \\ &\stackrel{(b)}{\approx} \mathbb{E}_{I,s} \left[\left(1 - (1 - e^{-s(\sigma^2 + I)\zeta_\rho})^{M_\rho} \right)^b \right] \\ &\stackrel{(c)}{=} \mathbb{E}_{I,s} \left[\sum_{\tau_1=0}^b \binom{b}{\tau_1} \left(- (1 - e^{-s(\sigma^2 + I)\zeta_\rho})^{M_\rho} \right)^{\tau_1} \right] \\ &\stackrel{(d)}{=} \mathbb{E}_{I,s} \left[\sum_{\tau_1=0}^b \sum_{\tau_2=0}^{M_\rho \tau_1} \binom{b}{\tau_1} \binom{M_\rho \tau_1}{\tau_2} (-1)^{\tau_1 + \tau_2} \exp(-s\sigma^2 \zeta_\rho \tau_2) \right. \\ &\quad \left. \prod_{j=1}^K \mathcal{L}_{I_j,L}(s\zeta_\rho \tau_2) \mathcal{L}_{I_j,N}(s\zeta_\rho \tau_2) \right] \end{aligned} \quad (67)$$

where (a) follows from $\Gamma(s) = \gamma(s, x) + \Gamma(s, x)$, (b) is from that the CDF of a Gamma random variable can be tightly upper bounded by $\frac{\gamma(M_\rho, s(I+\sigma^2))}{\Gamma(M_\rho)} < [1 - e^{-s(I+\sigma^2)\zeta_\rho}]$, (c) and (d) follows from the binomial expansion theorem, the definition of the Laplace transform of the interference and the noise and $\mathcal{L}(s) = \exp(-s\sigma^2) \prod_{j=1}^K \mathcal{L}_{I_{j,L}}(s) \mathcal{L}_{I_{j,N}}(s)$.

Since the PDF of the $L_{k,\rho}$ is obtained in (14), the proof of Theorem 2 can be completed by averaging over $L_{k,\rho}$.

F. Proof of Theorem 3

Given that u_0 is associated with a LOS/NLOS BS in the k th tier, the mean local delay can be derived as

$$\begin{aligned} \xi_{-1,k,\rho} &= \mathbb{P} \left(\frac{P_k G_0 h_{k,0} L_k^{-1}(r)}{\sigma^2 + I} > \theta \right)^{-1} \\ &= \mathbb{E}_{I,s} \left[\left(1 - \frac{\gamma(M_\rho, s(\sigma^2 + I))}{\Gamma(M_\rho)} \right)^{-1} \right] \\ &\approx \mathbb{E}_{I,s} \left[\left(1 - \left(1 - e^{-s(\sigma^2 + I)\zeta_\rho} \right)^{M_\rho} \right)^{-1} \right] \\ &\stackrel{(a)}{=} \mathbb{E}_{I,s} \left[\sum_{\tau_1=0}^{\infty} (-1)^{\tau_1} \left(- \left(1 - e^{-s(\sigma^2 + I)\zeta_\rho} \right)^{M_\rho} \right)^{\tau_1} \right] \quad (68) \\ &= \mathbb{E}_{I,s} \left[\sum_{\tau_1=0}^{\infty} \sum_{\tau_2=0}^{M_\rho \tau_1} \binom{M_\rho \tau_1}{\tau_2} (-1)^{\tau_2} e^{-s\sigma^2 \zeta_\rho \tau_2} \right. \\ &\quad \left. \prod_{j=1}^K \mathcal{L}_{I_{j,L}}(s \zeta_\rho \tau_2) \mathcal{L}_{I_{j,N}}(s \zeta_\rho \tau_2) \right] \end{aligned}$$

where (a) follows from the binomial theorem for a negative integer power $(x + y)^n = \sum_{\tau=0}^{\infty} (-1)^\tau \binom{-n+\tau-1}{\tau} y^{n-\tau} x^\tau$.

REFERENCES

- [1] A. Gupta and R. K. Jha, "A survey of 5G network: Architecture and emerging technologies," *IEEE Access*, vol. 3, pp. 1206-1232, 2015.
- [2] P. Schulz et al., "Latency critical IoT applications in 5G: Perspective on the design of radio interface and network architecture," *IEEE Commun. Mag.*, vol. 55, no. 2, pp. 70-78, Feb. 2017.
- [3] T. S. Rappaport et al., "Millimeter wave mobile communications for 5G cellular: It will work!" *IEEE Access*, vol. 1, pp. 335-349, 2013.
- [4] X. Wang, L. Kong, F. Kong, F. Qiu, M. Xia, S. Arnon, and G. Chen, "Millimeter wave communication: a comprehensive survey," *IEEE Commun. Surveys Tuts.*, vol. 20, no. 3, pp. 1616-1653, Aug. 2018.
- [5] H. S. Dhillon, R. K. Ganti, F. Baccelli, and J. G. Andrews, "Modeling and analysis of K-tier downlink heterogeneous cellular networks," *IEEE J. Sel. Areas Commun.*, vol. 30, no. 3, pp. 550-560, Apr. 2012.
- [6] H.-S. Jo, Y. J. Sang, P. Xia, and J. G. Andrews, "Heterogeneous cellular networks with flexible cell association: A comprehensive downlink SINR analysis," *IEEE Trans. Wireless Commun.*, vol. 11, no. 10, pp. 3484-3495, Oct. 2012.
- [7] H. Elsayy, E. Hossain, and M. Haenggi, "Stochastic geometry for modeling, analysis, and design of multi-tier and cognitive cellular wireless networks: A survey," *IEEE Commun. Surveys Tuts.*, vol. 15, no. 3, pp. 996-1019, Jun. 2013.
- [8] A. Damnjanovic et al., "A survey on 3GPP heterogeneous networks," *IEEE Wireless Commun. Mag.*, vol. 18, no. 3, pp. 10-21, Jun. 2011.
- [9] M. Di Renzo, A. Guidotti, and G. E. Corazza, "Average rate of downlink heterogeneous cellular networks over generalized fading channels: A stochastic geometry approach," *IEEE Trans. Commun.*, vol. 61, no. 7, pp. 3050-3071, Jul. 2013.
- [10] M. Di Renzo, "Stochastic geometry modeling and analysis of multi-tier millimeter wave cellular networks," *IEEE Trans. Wireless Commun.*, vol. 14, no. 9, pp. 5038-5057, 2015.
- [11] T. Bai and R. W. Heath, "Coverage and rate analysis for millimeter-wave cellular networks," *IEEE Trans. Wireless Commun.*, vol. 14, no. 2, pp. 1100-1114, 2015.
- [12] X. Yu, J. Zhang, M. Haenggi, and K. B. Letaief, "Coverage analysis for millimeter wave networks: the impact of directional antenna arrays," *IEEE J. Sel. Areas Commun.*, vol. 35, no. 7, pp. 1498-1512, Jul. 2017.
- [13] H. Shokri-Ghadikolaei, C. Fischione, G. Fodor, P. Popovski, and Michele Zorzi, "Millimeter wave cellular networks: a MAC layer perspective," *IEEE Trans. Commun.*, vol. 63, no. 10, pp. 3437-3458, Oct. 2015.
- [14] E. Turgut and M. C. Gursoy, "Coverage in heterogeneous downlink millimeter wave cellular networks," *IEEE Trans. Commun.*, vol. 65, no. 10, pp. 4463-4477, Oct. 2017.
- [15] C. Skouroumounis, C. Psomas, and I. Krikidis, "Low-complexity base station selection scheme in mmWave cellular networks," *IEEE Trans. Commun.*, vol. 65, no. 9, pp. 4463-4477, Sep. 2017.
- [16] D. Maamari, N. Devroye, and D. Tuninetti, "Coverage in mmWave cellular networks with base station cooperation," *IEEE Trans. Wireless Commun.*, vol. 15, no. 4, pp. 2981-2994, Apr. 2016.
- [17] S. Singh, M. N. Kulkarni, A. Ghosh, and J. G. Andrews, "Tractable model for rate in self-backhauled millimeter wave cellular networks," *IEEE J. Sel. Areas Commun.*, vol. 33, no. 10, pp. 2196-2211, 2015.
- [18] H. Elshaer, M. N. Kulkarni, F. Boccardi, J. G. Andrews, and M. Dohler, "Downlink and uplink cell association with traditional macrocells and millimeter wave small cells," *IEEE Trans. Wireless Commun.*, vol. 15, no. 9, pp. 6244-6258, Sep. 2016.
- [19] M. Haenggi, "The meta distribution of the SIR in Poisson bipolar, and cellular networks," *IEEE Trans. Wireless Commun.*, vol. 15, no. 4, pp. 2577-2589, Apr. 2016.
- [20] Y. Wang, M. Haenggi, and Z. Tan, "SIR Meta distribution of K-tier downlink heterogeneous cellular networks with cell range expansion," *IEEE Trans. Wireless Commun.*, vol. 67, no. 4, pp. 3069-3081, Apr. 2019.
- [21] S. Kalamkar and M. Haenggi, "Simple approximations of the SIR meta distribution in general cellular networks," *IEEE Trans. Commun.*, vol. 67, no. 6, pp. 4393-4406, Jun. 2019.
- [22] M. Salehi, A. Mohammadi, and M. Haenggi, "Analysis of D2D underlaid cellular networks: SIR meta distribution and mean local delay," *IEEE Trans. Commun.*, vol. 65, no. 7, pp. 2904-2916, Jul. 2017.
- [23] Q. Cui, X. Yu, Y. Wang, and M. Haenggi, "The SIR meta distribution in Poisson cellular networks with base station cooperation," *IEEE Trans. Commun.*, vol. 66, no. 3, pp. 1234-1249, Mar. 2018.
- [24] M. Salehi, H. Tabassum, and E. Hossain, "Meta distribution of SIR in large-scale uplink and downlink NOMA networks," *IEEE Trans. Commun.*, vol. 67, no. 4, pp. 3009-3025, Apr. 2019.
- [25] Y. Wang, M. Haenggi, and Z. Tan, "The Meta distribution of the SIR for cellular networks with power control," *IEEE Trans. Commun.*, vol. 66, no. 4, pp. 1745-1757, Apr. 2018.
- [26] N. Deng and M. Haenggi, "A fine-grained analysis of millimeter-wave device-to-device networks," *IEEE Trans. Commun.*, vol. 65, no. 11, pp. 4940-4954, Nov. 2017.
- [27] H. Ibrahim, H. Tabassum, and U. T. Nguyen, "The meta distributions of the SIR/SNR and data rate in coexisting sub-6GHz and millimeter-wave cellular networks" *arXiv preprint arXiv:1905.12002*, 2019.
- [28] F. Baccelli and B. Blaszczyzyn, "Stochastic geometry and wireless networks: Volume II applications," *Found. Trends Netw.*, vol. 4, nos. 1-2, pp. 1-312, 2010.
- [29] A. Thornburg, T. Bai, and R. W. Heath, "Performance analysis of mmWave ad hoc networks," *IEEE Trans. Signal Process.*, vol. 64, no. 15, pp. 4065-4079, Aug. 2016.
- [30] T. Bai and R. W. Heath, "Coverage and rate analysis for millimeterwave cellular networks," *IEEE Trans. Wireless Commun.*, vol. 14, no. 2, pp. 1100-1114, Feb. 2015.
- [31] J. Wildman, P. H. J. Nardelli, M. Latva-aho, and S. Weber, "On the joint impact of beamwidth and orientation error on throughput in directional wireless Poisson networks," *IEEE Trans. Wireless Commun.*, vol. 13, no. 12, pp. 7072-7085, Dec. 2014.
- [32] M. Salehi, A. Mohammadi, and M. Haenggi, "Analysis of D2D underlaid cellular networks: SIR meta distribution and mean local delay," *IEEE Trans. Commun.*, vol. 65, no. 7, pp. 2904-2916, Jul. 2017.
- [33] I. S. Gradshteyn and I. M. Ryzhik, *Table of Integrals, Series, and Products*. New York, NY, USA: Academic, 2014.
- [34] C. Li, J. Zhang, J. G. Andrews, and K. B. Letaief, "Success probability and area spectral efficiency in multiuser MIMO HetNets," *IEEE Trans. Commun.*, vol. 64, no. 4, pp. 1544-1556, Apr. 2016.
- [35] P. Henrici, *Applied and Computational Complex Analysis, Volume 1: Power Series Integration Conformal Mapping Location of Zero*, vol. 1. Hoboken, NJ, USA: Wiley, 1988.

- [36] C. Li, J. Zhang, and K. B. Letaief, "Throughput and energy efficiency analysis of small cell networks with multi-antenna base stations," *IEEE Trans. Wireless Commun.*, vol. 13, no. 5, pp. 2505-2517, May 2014.
- [37] A. K. Gupta, H. S. Dhillon, S. Vishwanath, and J. G. Andrews, "Down-link multi-antenna heterogeneous cellular network with load balancing," *IEEE Trans. Commun.*, vol. 62, no. 11, pp. 4052-4067, Nov. 2014.
- [38] J. Wen, K. Huang, S. Yang, and V. O. K. Li, "Cache-enabled heterogeneous cellular networks: Optimal tier-level content placement," *IEEE Trans. Wireless Commun.*, vol. 16, no. 9, pp. 5939-5952, Sep. 2017.